Stem Hydraulic Conductivity depends on the Pressure at Which It Is Measured and How This Dependence Can Be Used to Assess the Tempo of Bubble Pressurization in Recently Cavitated Vessels[1][OPEN]

Yujie Wang, Jinyu Liu, and Melvin T. Tyree*

College of Forestry, Northwest A & F University, Yangling, Shaanxi 712100, China

ORCID ID: 0000-0002-3729-2743 (Y.W.).

Cavitation of water in xylem vessels followed by embolism formation has been authenticated for more than 40 years. Embolism formation involves the gradual buildup of bubble pressure (air) to atmospheric pressure as demanded by Henry's law of equilibrium between gaseous and liquid phases. However, the tempo of pressure increase has not been quantified. In this report, we show that the rate of pressurization of embolized vessels is controlled by both fast and slow kinetics, where both tempos are controlled by diffusion but over different spatial scales. The fast tempo involves a localized diffusion from endogenous sources: over a distance of about 0.05 mm from water-filled wood to the nearest embolized vessels; this process, in theory, should take <2 min. The slow tempo involves diffusion of air from exogenous sources (outside the stem). The latter diffusion process is slower because of the increased distance of diffusion of up to 4 mm. Radial diffusion models and experimental measurements both confirm that the average time constant is >17 h, with complete equilibrium requiring 1 to 2 d. The implications of these timescales for the standard methods of measuring percentage loss of hydraulic conductivity are discussed in theory and deserve more research in future.

Vulnerability curves (VCs) have been used as a measure of drought resistance of woody plants, and many methods have been used and evaluated to construct VCs (Cochard et al., 2013). Vessels cavitate in response to increasing drought stress and immediately fill with a mixture of water vapor and air. Henry's law of gas solubility in water demands that, eventually, the air pressure in an embolized vessel will equal atmospheric pressure provided that the surrounding water pressure remains low enough. Most presumed, until recently, that the air pressure builds up to atmospheric pressure in 10 to 20 min (Sperry and Tyree, 1988; Tyree and Zimmermann, 2002). In contrast, research has shown that dissolving of air bubbles in stem takes many hours (10–100) depending on water pressure applied and stem diameter (Tyree and Yang, 1992; Yang and Tyree, 1992), but how long it takes to fully embolize a vessel remains unknown. Recently, cavitron methods have been developed to estimate average bubble pressure by measuring the impact of the water tension on stem hydraulic conductivity when the water pressure adjacent to a bubble changes, causing bubble expansion or compression (Wang et al., 2014b, 2015).

Subatmospheric bubble pressure in vessels makes the measurements of hydraulic conductivity of stems, k_h, inaccurate when measured at or near atmospheric pressure, because bubble collapse will cause an increase in k_h as shown by traditional measurements (Table I; Tyree and Yang, 1992; Yang and Tyree, 1992) and modern cavitron methods (Wang et al., 2015). Intuitively, if embolized vessels have subatmospheric air pressure, then the air bubbles ought to collapse in volume as the surrounding water tension increases to zero (atmospheric pressure). A collapsing air bubble will result in a vessel partly filled with water, and a partly water-filled vessel is capable of conducting water if it contacts adjacent water-filled vessels. Bubble pressure will also increase with time because of Henry's law, and the time required to fully embolize the vessels depends on the penetration rate of air through the xylem as governed by Fick's law of diffusion. Where does the air come from, and how long does it take to fully embolize a vessel?

To answer the questions, some insights can be gained through some theoretical analyses and calculations before conducting experiments. Embolized vessels serve as a sink of air, and there are two main sources of air: (1) an endogenous source, which is the air dissolved in liquid phase inside the stem, and (2) an exogenous source, which is the air in atmospheric phase outside the stem. Air dissolved in water in the stem would be drawn out very quickly to fill recently cavitated vessels because of the very short distance between newly cavitated vessels

[1] This work was supported by 1000 Talents (5-year research grant to M.T.T.).

* Address correspondence to mel.tyree@cantab.net.

The author responsible for distribution of materials integral to the findings presented in this article in accordance with the policy described in the Instructions for Authors (www.plantphysiol.org) is: Melvin T. Tyree (mel.tyree@cantab.net).

Y.W. and M.T.T. designed the experiment and devised the theory; Y.W. and J.L. conducted the experiments; M.T.T. wrote the article with frequent consultation with Y.W.

[OPEN] Articles can be viewed without a subscription.

www.plantphysiol.org/cgi/doi/10.1104/pp.15.00875

Table I. *Table of abbreviations*

Abbreviation	Meaning
D, D_w	Coefficient of diffusion of gas in water and wood, respectively
k_h	Hydraulic conductivity of the stem
k_{max}	Maximum hydraulic conductivity of the stem
L_v, L_b	Length of vessel and bubble, respectively
τ	Time constant in an exponential process
T	Tension in xylem
T_c	Central tension in stem that spins in a centrifuge
PLC	PLC of stem
P_{50}, P_{63}	Xylem pressure when stem loss is 50% or 63% of its maximum conductivity, respectively
VC	Vulnerability curve
Cavitron	Cochard's cavitron (Cochard rotor) that both spins stem and measures conductivity in the centrifuge
Sperry rotor	Standard centrifuge method that spins stem in the centrifuge and measures k_h in conductivity apparatus out of the centrifuge
P_b*	Bubble pressure in stem before bubble collapse

and the surrounding water. For example, if one-half of the vessels cavitate quickly, the approximate distance between cavitation voids will be 0.05 mm (Wang et al., 2015), but ambient air beyond the bark boundary has to move a comparatively long way (many millimeters) into the cavitated vessels through the bark and wood. The reason for the longer time for exogenous air to move follows from the relationship between the median distance that a molecule can diffuse, x, and the time for the diffusion, t. The relationship is $x^2 = 2Dt$, where D is the diffusion coefficient of air molecules in water. In a recent article (Wang et al., 2015), it was argued that the time for endogenous bubble pressure equilibrium was ≤10 s over diffusional distances of 0.05 to 0.1 mm. Hence, it follows that, if distances are 10^2 more, the time will be 10^4 more for diffusion from exogenous sources (i.e. 1–2 d versus 10 s). However, Wang et al. (2015) used an inappropriate value for D equal to air diffusion in pure water. Using a more appropriate value actually measured in wood (Sorz and Hietz, 2006), the recomputed time is nearly 1 min (Supplemental Fig. S1; Supplemental Theory S1). The original model (Wang et al., 2015) has not changed, except for the use of a more accurate value of D. However, the qualitative argument that some bubble pressurization is fast and that the rest is slow is still correct.

It could be argued theoretically that, based on Fick's law of diffusion, the ideal gas law of air bubbles, and Henry's law of solubility of air in water, the time for exogenous bubble pressure equilibrium could be even more than 1 d. However, a technically valid, experimental verification of equilibrium time constant is always preferable to theory alone. Hence, the objective of this study is to first measure experimentally the time constant of exogenous equilibration and second, explain by theory why the time constant should be the value measured experimentally.

Readers should consult the work by Wang et al. (2015) for details about the theoretical and experimental approaches used in this study, but the basic idea is easy to explain without rigorous theory. It is well known that stem k_h increases if bubbles dissolve or otherwise grow smaller (Tyree and Yang, 1992; Yang and Tyree, 1992); therefore, information about bubble size or pressure can be deduced from repeated measurements of k_h. In brief, bubbles in vessels can be compressed when bubble pressure is lower than the sum of water pressure and capillary pressure, and water will partly refill the vessel as bubbles collapse. Partly refilled vessels enhance stem conductivity provided that the water is in contact through pit membranes with adjacent water-filled vessels. In this article, we use a centrifuge technique (Wang et al., 2014b) to manipulate the water pressure or tension, T, adjacent to embolized vessels. If the initial bubble pressure, P_b*, is low, the bubbles will collapse more as tension decreases toward zero than if P_b* is high. Wang et al. (2015) showed that P_b* can be computed by fitting functions of k_h versus T in a cavitron. Hence, by doing repeated measurements over many hours of k_h versus T, one can determine the tempo of P_b* change.

RESULTS

Transients in k_h Values after a Change in T_c

The accurate determination of bubble pressure requires the accurate evaluation of k_h at two or more T_c values. When T_c is adjusted from very high values, which cause cavitation and minimum k_h, to very low values, which cause bubble collapse, an increase in k_h occurs; there is a transient period when extra water has to flow into the stem segment to partly fill the vessel lumen as the bubbles collapse. Wang et al. (2015) reported that this could take up to 30 min, and therefore, it is appropriate to give specific proof here.

Examples of the transients are shown in Figure 1. Figure 1A shows a typical transient process when T_c dropped to 0.0565 MPa in one step; Figure 1B shows the combination of 32 transient processes of *Populus alba* × *Populus glandulosa* 'Uyeki' (hereafter referred to as *Populus* 84K), and the transient followed a dual-exponential curve fitted by $y = 0.506e^{-t/9.9} + 0.480e^{-t/1.85} + 1.001$, where t = time in minutes in the x axis, and the denominator of t is the time constant, τ, for equilibration.

The stem segment releases water when T_c increases from the minimum tension to a higher one as bubble expands, and as a result, k_h measured immediately after the increase of tension would be underestimated as shown in Figure 1C. The wait time before a stable k_h can be measured and was usually less than 10 min for those points obtained after increasing tensions to construct a multipoint curve. Typically, the time required to measure a multipoint curve was about 1.10 ± 0.23 h (mean ± SD; Wang et al., 2015).

Two-Point Estimation of Bubble Pressure (P_b*) at High Tension

Bubble pressure could be determined in less time with sufficient accuracy by collecting only two points.

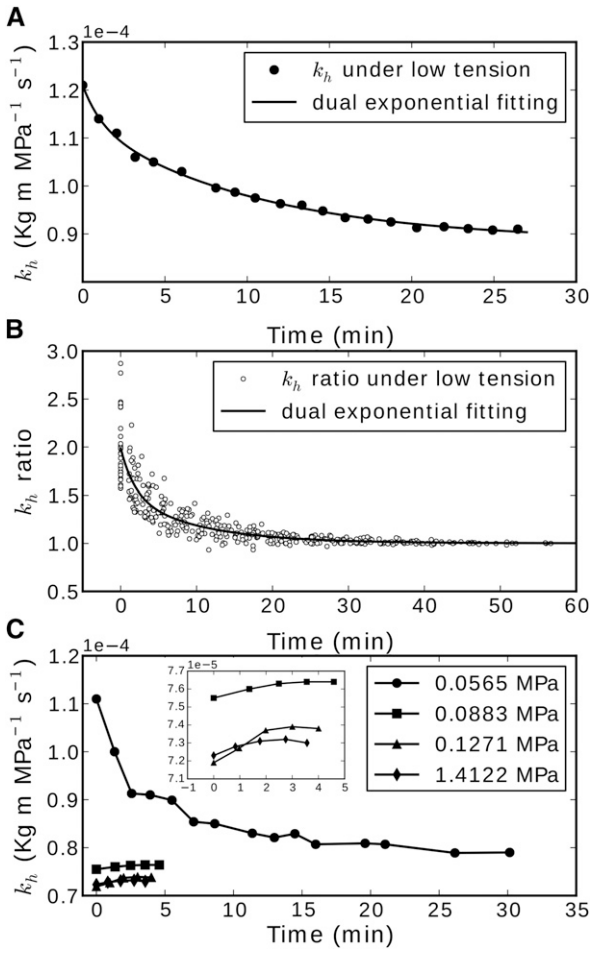

Figure 1. Examples of transient k_h values caused by water absorption in stems in a cavitron after reduction from high T_c to the lowest T_c at 800 rpm. A, Kinetics of k_h measurement while a stem absorbs water from reservoirs in a typical experiment. B, The combined kinetics of $n = 32$ experiments; to combine curves, k_h had to be normalized to the equilibrium k_h (ratio equal to 1 at equilibrium). The kinetics can be fitted by a dual-exponential curve. C illustrates the kinetics to obtain stable k_h after the transition from maximum T_c to minimum T_c (0.0565 MPa) and then higher tensions. The transition times when T_c is subsequently increased to 0.0883, 0.1271, and 1.4122 in steps are quite short by comparison.

The hydraulic recovery model (Wang et al., 2015) was used to estimate the average bubble pressure in the stem using a multipoint curve. However, a multipoint curve is not essential to compute P_b*. At its simplest level, the ideal gas law can be used to compute the length of the bubble. At highest tension, the length of the bubble equals the vessel length, L_v, and at lower tension, the higher P_b corresponds to a lower bubble length, L_b. The ratio of lengths is governed by the ideal gas law and Henry's law; the former relates bubble pressure to bubble length (P_b*:$P_b = L_b$:L_v), and the latter law relates bubble pressure to gas concentration in adjacent fluid through a proportionality constant. The value of k_h can be expressed as a function of L_b (Wang et al., 2015). The multipoint curve fitting slightly increased the accuracy of the estimation of k_h, but a sufficiently accurate value can be deduced by two widely separated points in the same way that the pressure of a compressed gas in a cylinder and piston can be deduced from knowing one pressure and two lengths analogous to P_b, L_v, and L_b. To reduce the time for determination of bubble pressure, a simplified two-point method was used to do the fitting; the two points were for the highest (where embolism is induced) and lowest T_c values (0.0565 MPa).

The two-point method for the estimation of bubble pressure, P_b*, was not significantly different from that of the multipoint method (Fig. 2; paired Student's t test, $P = 0.28$). The advantages of using two points were faster measurement and less perturbation of the system. The perturbation results, because while measuring conductance at low tension, the driving force for diffusion of gases into the bubble decreases because of the rise in pressure of the bubble. Hence, while measuring the bubble pressure, the rate of increase of the pressure is reduced, modifying the outcome of future measurements. The time needed for measuring two points at high tension and lowest tension was 0.62 ± 0.19 h (mean ± SD), reducing the experimental time by nearly a factor of 2.

Relationship between Percentage Loss of Conductivity at High Tension and Bubble Pressure

The initial bubble pressure in stems (that had spun for 20 min under high tension and equilibrated at the lowest tension for more than 30 min) was positively correlated with percentage loss of conductivity (PLC)

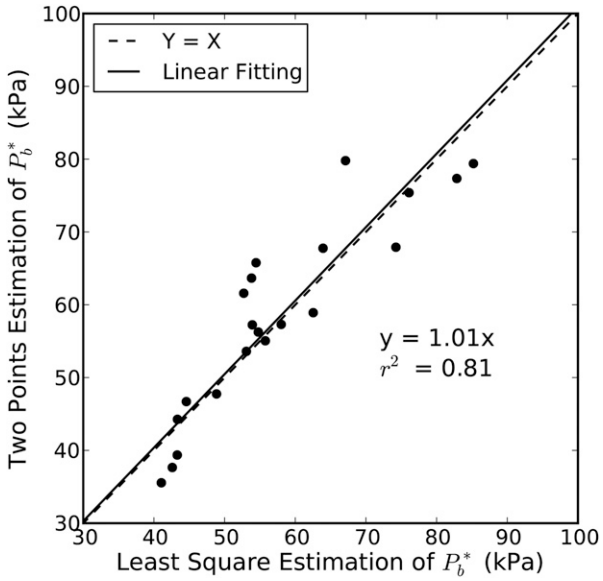

Figure 2. Comparison of bubble pressure derived by two different methods: the x axis shows the least-square fitting of a multipoint curve, and the y axis shows bubble pressure computed from the two most extreme points. The values of P_b* obtained by the two methods did not differ significantly ($P = 0.28$; i.e. the slope was not significantly different from 1).

for both *Acer mono* and *Populus* 84K as shown in Figure 3. For both species, the PLC correlated positively with the initial bubble pressure. Also, the lowest bubble pressure was approximately 40 kPa. The slopes and intercepts of two species were different, indicating a difference in bubble pressurization kinetics, which might result from the differences in the physical structure (anatomy) of the two species. Stems with 80% PLC had average bubble pressure around 70 kPa in both species as predicted from the linear fitting. A possible reason for this surprising trend will be covered in "Discussion." Note that the initial bubble pressures (after 0.6 h) were consistently higher than might be predicted from endogenous sources of air (figure 1 in Wang et al., 2015); the reason for this will be explained in "Discussion."

Tempo of Bubble Formation in Recently Cavitated Vessels

The time constant, τ, for the progression of bubble pressure toward atmospheric pressure was quite long in recently cavitated vessels, and the time required was independent of the PLC of the stem. Figure 4 shows the typical progress of bubble pressurization versus the accumulated time at both high and low tensions. Exponential fitting ($y = A_b - A_0 e^{-x/\tau}$) is used to fit the bubble pressurization, and it gives an estimate of the exponential time constant, where A_b = the equilibrium barometric pressure (100 kPa), and $A_b - A_0$ is the initial pressure at 1 h after the cavitation. We used plots of time versus P_b* to generate a τ and used τ to compute the one-half and 99% equilibrium times.

There was no significant correlation between PLC and τ as shown in Figure 5 ($P = 0.17$); the mean ± SE was 17.1 ± 3.3 h. Additionally, the computed one-half and 99% formation times can be computed by $T_{50} = \ln(2) \cdot \tau$ and $T_{99} = \ln(100) \cdot \tau$, respectively. Experimental results showed that the mean T_{50} of *Populus* 84K was around 11.9 ± 2.3 h and that the mean T_{99} was 78.7 ± 15.0 h.

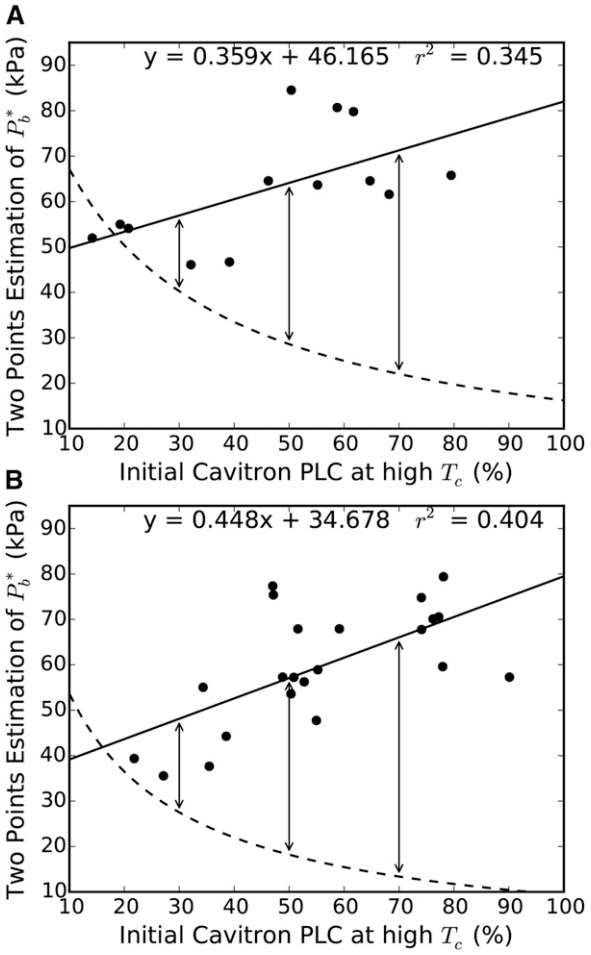

Figure 3. Relationship between initial stem PLC measured in a cavitron and initial bubble pressure measured within 0.5 h of cavitation. The *x* axis is the PLC of stem at high tension where embolism is induced, and the *y* axis is the estimated bubble pressure derived from the two-point method. A shows the results of *A. mono*, and B shows the results of *Populus* 84K. The dashed lines show the theoretical endogenous equilibrium bubble pressures from Henry's law that occur in 2 min or less time after the cavitation events. Double-headed arrows show the changes that occur by 1 h after the cavitation events.

DISCUSSION

Influence of Initial PLC Profiles on Computation of Bubble Pressure (Curve Fitting)

In Wang et al., 2015, curve fitting was done assuming that the embolized vessel fraction (ε) in stems was independent of position in a cavitron. This is impossible to prove, but based on measurements outside a cavitron (Cai et al., 2010), it seems likely that some kind of quadratic function would be expected like that in Figure 6A. Figure 6A shows a flat ε-distribution and two quadratic distributions, all of which yield the same theoretical PLC for the whole stem spinning in a cavitron. Figure 6B shows the theoretical impact of these different distributions on how k_h changes with T_c based on the models in Wang et al., 2015 for a P_b* of 50 kPa. It can be inferred from Figure 6 that the most variable ε-distribution (Quad1) resulted theoretically in the flattest trend in the tension range from 0.1 to 1 MPa. Therefore, one advantage of using a two-point estimation of bubble pressure at low tension (arrow at 0.0565 MPa in Fig. 6B) and high tension (arrow at 2 MPa in Fig. 6B) is that bubble pressure is approximately independent of the shape of the PLC distribution (Fig. 6A), because at the low tensions, quad 1 and quad 2 distributions differ only 2.5% and 1.7%, respectively, in hydraulic conductivity from flat distribution. Also, the estimated bubble pressures of the three distributions (flat, quad 1, and quad 2) differed slightly: 48.96, 51.07, and 50.41 kPa, respectively.

The ε-distribution in stems reported in Cai et al., 2010 was measured at water pressure equal to 1 or 2 kPa above atmospheric pressure. Under these conditions, an approximately quadratic distribution was found.

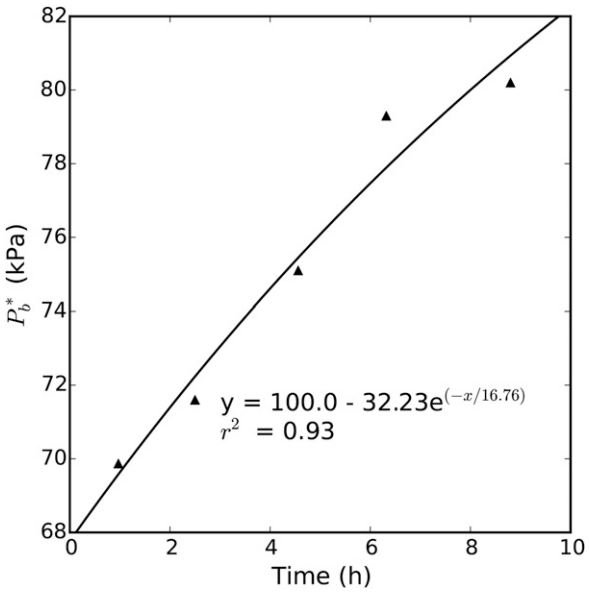

Figure 4. An example of the tempo of bubble pressure increase of *Populus* 84K: the time on the *x* axis is the accumulated time that the stem was under both high and low tensions; the *y* axis is P_b* at each *x* axis time. An exponential curve is approximately linear at the beginning of an exponential, and the time constant for the early part of the exponential can be accurately determined by the linear phase; it agrees with theoretical expectations (see discussion connected with Fig. 8).

Based on the results of this study and in the article by Wang et al. (2015), we think that the quadratic distribution will be different while the stem is spinning from that reported in Cai et al., 2010, because the subatmospheric bubble pressure in cavitated vessels is altered after the stem is removed from a centrifuge. The results of this study suggest a way of estimating the actual distribution, albeit somewhat crudely. The approach for a future study would be to obtain a multipoint curve of k_h versus T_c like that in Figure 6B. The curve fitting can be done in two stages to determine both P_b* and the PLC distribution (Fig. 6B). In the first stage, P_b* is calculated based on values of k_h at the locations of the arrows in Figure 6B. Then, the root mean square error of a multipoint fit would be minimized using different quadratic ε-distributions until the fit is optimized. In the future, this might provide a crude estimate of the ε-distribution while the stem is spinning. In this article, the theoretical impact of ε-distribution on P_b* was avoided by using the two-point method to calculate P_b*.

Best Estimation of Bubble Pressure and Other Implications

Water absorption and release affect the k_h measurements by the influence of bubble collapse or expansion on the inflow or outflow rate; hence, experiments must be designed to account for the time for transient flows to finish. In addition, the two-point method was deemed preferable to save time and get better estimation of the time required for the kinetics of P_b* increase. The two-point method saved 0.48 h per pressure determination. The longest time for the transient in k_h was when stepping down from the highest T_c to the lowest T_c (0.0565 MPa; about 30 min). The stepwise increases in T_c resulted in relatively faster equilibration times (5 min; Fig. 1B). As a consequence, the time saved in collecting a two-point estimation of bubble pressure (Fig. 2) versus a multipoint curve estimation of pressure was a factor of 2.

The kinetics of change of k_h reported here within a cavitron are not new, because they have been reported outside a cavitron as well. Those who use the Sperry rotor to induce embolism and a conductivity apparatus to measure k_h have routinely noticed a transient in k_h, which has been attributed to the extreme desiccation of the stem segments after spinning them in the cavitron (U. Hacke, personal communication). In our view, the reason for the transient in k_h is bubble collapse rather than stem swelling because woody stems are quite rigid and cannot change much in volume, but bubble volume changes are comparatively large. However, water flow to swell dehydrated bark will contribute more than the woody parts of stems. These statements about swelling of bark versus stems follow from precise measurements of diurnal stem diameter change using linear voltage displacement transducers and relating stem diameter to stem water potential. Most of the volume change of stems is in the bark rather than in the wood, and the volume changes of whole stems are less than 0.03% versus several percentages for the volume of bubble collapse, which will happen independently of stem volume change (Irvine and Grace, 1997). Even in crop species, the volume change of stems is much smaller than the water content changes (Zhou et al., 2015). The traditional way to deal with the rehydration kinetics or change in k_h with time is to measure the rehydration rate of the stem with no applied pressure and then correct the flow rate measured with an applied pressure for the rehydration rate (Hacke et al., 2000; Torres-Ruiz et al., 2012).

Sources of Air in the Cavitated Vessels Influencing Initial Bubble Pressure and the Kinetics of Bubble Pressure in the First 0.5 h: A Reevaluation

In the original article in this series, Wang et al. (2015) theorized that there ought to be two sources of air for bubble formation in recently cavitated vessels. The essence of the idea is alluded to in the introduction, and the details are explained in Wang et al., 2015. The endogenous air dissolved in surrounding water adjacent to the cavitated vessel can equilibrate quickly with the water vapor-filled void, because the time for diffusion over short distances (0.04–0.08 mm) is approximately 2 min or less for the local equilibrium (Supplemental Fig. S1). In contrast, for exogenous air beyond the bark, diffusion time increases with the distance squared, and hence, equilibration times approaching 1 d are to be expected. The latter prediction is supported by Figure 4 and the extrapolated equilibration time of 29 h ("Results").

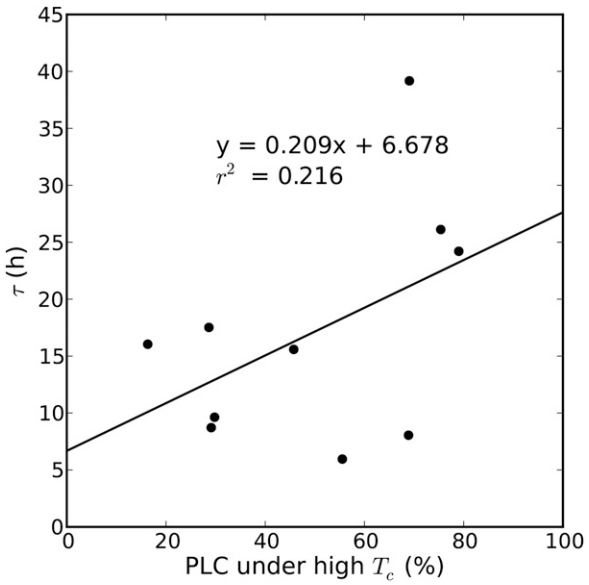

Figure 5. This plot shows the relationship between initial cavitron PLC and exponential time constant, τ, for the kinetics of increase in bubble pressure. PLC (x axis) is the induced PLC in the stem under high tension, and τ (y axis) is the time constant derived from the exponential fit of the P_b* curve in Figure 4. The mean ± SE is 17.0 ± 3.4 h for all values in this plot. The slope is not significantly different from 0 (P = 0.17).

The observations in Figure 3 illustrate the combined role of endogenous and exogenous sources of gas to explain events in the first 1 h or less. The experimental data in Figure 3 show the observed P_b* values (circles and regression lines in Fig. 3) and the contribution of endogenous sources from the application of Henry's law equilibration with endogenous sources of air within 1 min (dashed lines in Fig. 3). The connection between Henry's and Fick's laws is straightforward if the reader remembers that P_b* is a proxy for air concentration in the water adjacent, C_a, to the bubble.

From Henry's law, we have that $C_a = k_a \times P_b{*}t$, where k_a = Henry's law constant. Hence, to understand the deviations between Henry's law equilibration in 1 min and the status after about 60 min, we need to invoke the appropriate value for D_w and a cylindrical diffusion model.

For an initial PCL of 50%, the rapid endogenous equilibration by Henry's law in the first 1 min (Wang et al., 2015) accounts for bubble pressures 25 and 32 kPa for *Populus* 84K and *A. mono*, respectively, based on the dashed lines in Figure 3. In comparison, the actual values were about 57 and 64 kPa based on the regression lines in Figure 3. The remainders of the increases are accounted for by radial diffusion of exogenous air in the next 1 h. Fick's law diffusion for a cylinder would account for this extra pressurization in the first 1 mm or less from the surface of the stem.

Exogenous Sources: Radial Diffusion across the Xylem

The exogenous source of air can be modeled as diffusion through cylindrical shells across the radius of a branch of the size used in our experiments. A similar cylindrical diffusion model was built to evaluate the radial diffusion of air through the xylem (details can be found in Supplemental Appendix S1, which shows a minor variation on the standard solutions found in Crank, 1979). Briefly, a cylindrical stem with bark, wood, and pith (external diameter of 4 mm) was divided into 20 thin cylindrical shells. The only deviation from the solution by Crank (1979) for cylinders is to allow localized Henry's law equilibration between water and gas phases evenly distributed throughout the wood. In our model, all of the shells share the same diffusion coefficient, D = 1.0E-6 cm^2 s^{-1}, measured in woody species (Sorz and Hietz, 2006). The diffusion

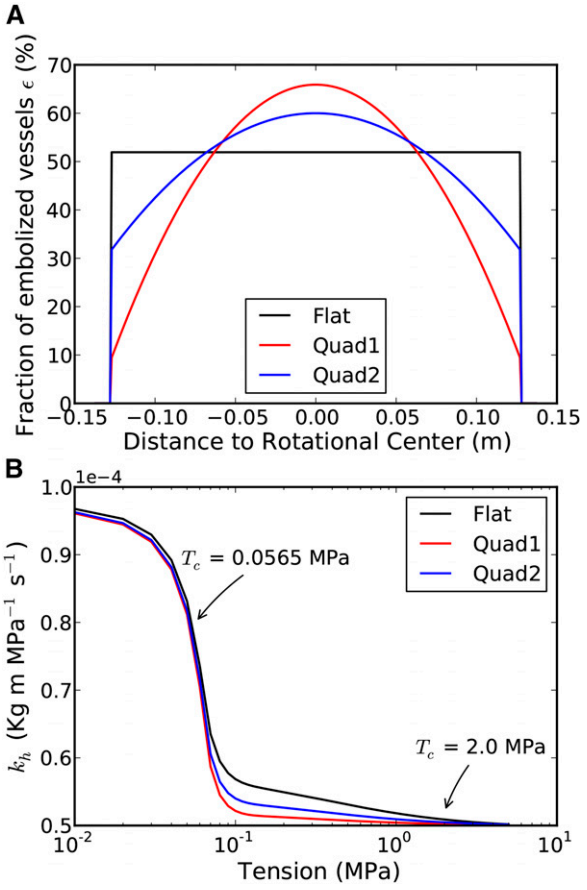

Figure 6. This figure shows the theoretical impact of PLC distribution in stem segments on the shape of hydraulic recovery curve. Hydraulic recovery curve is the plot of tension and hydraulic conductivity change caused by the collapse of bubbles in cavitated vessels versus tension. A shows three possible PLC distributions: one flat distribution ($y = y_c$) from −0.127 to 0.127 m, where y_c = 52.2, and two quadratic distributions $y = ax^2 + y_0$, where x is the distance from the location to the rotational axis, and a and y_0 are −3,500 and −1,750 and 65.9 and 60.0 for quad 1 and quad 2, respectively. The length of stem is 0.274 m, and the distance from the rotational axis to the water level is 0.127 m. B shows the hydraulic recovery curves of the three different PLC distributions, and the top arrow indicates the tension at 0.057 MPa. Maximum hydraulic conductivity is k_{max} = 1.0E-4 kg m MPa^{-1} s^{-1}, bubble pressure is P_b* = 50 kPa, capillary pressure is P_c = 12 kPa, and vessel length is L_v = 0.05 m.

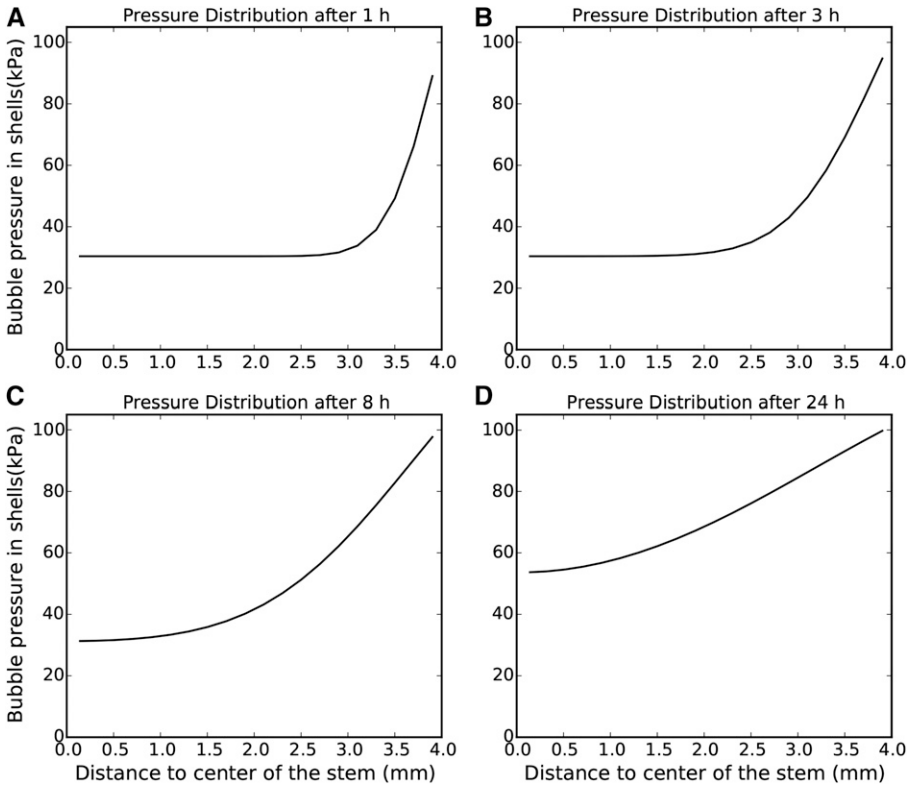

Figure 7. This plot shows the theoretical pressure distribution in 20 cylindrical shells of a woody stem. The external radius of the xylem was 4 mm. A to D show the pressure distributions (*y* axis) versus the radial distances to the center of different shells after 1, 3, 8, and 24 h, respectively.

coefficient of air is much lower in wood (1.0E-6 $cm^2\ s^{-1}$) than in pure water (2.0E-5 $cm^2\ s^{-1}$) because of the impact of the suberized walls of wood on diffusion of small molecules, such as O_2 and N_2. In our diffusion model across the xylem, we assume immediate equilibrium between water and bubble in each shell (for details, see Supplemental Appendix S1). Assuming a fraction of embolized water volume α = 0.05 and an initial equilibrated bubble pressure P_b* = 30 kPa, the model was run to estimate how fast bubbles pressurized versus radial position in the wood. Figure 7 shows the bubble pressure distribution after 1, 3, 8, and 24 h. Figure 8A shows the volume-weighted average bubble pressure in all of the shells (Fig. 8A, line), the average bubble pressures of the first three shells (Fig. 8A, dashed line), and that of the last three shells (Fig. 8A, dash-dot line). Figure 8B shows the first 60 h of the simulation in Figure 8A, plus it gives the time constant, τ, versus time. In cylindrical diffusion (Crank, 1979), the value of τ does not reach a constant value until about 30% from full equilibrium in terms of concentration of gases in water or in terms of bubble pressure or at about 20 h of time. Our longest experiments lasted about 9 h, with a mean ± SD = 7.5 ± 1.1 h of experimental time; and during this time, the final bubble pressure was 79.5 ± 0.4 kPa (equilibrium = 100). Our experimental results agree with the conclusions of theory (i.e. that 63% equilibrium occurs within 8 h after adjusting for the rapid endogenous equilibrium indicated by the dashed lines in Fig. 3). The theoretical tempo in Figure 8B would equal the experimental time if the value of D_w used in the model was increased by about 20% to 1.2E-6 (model results are not shown), which is still well within the range measured by Sorz and Hietz (2006) on many woody species.

It is obvious that the bubble pressures in those vessels nearer to the atmosphere (outer edge of the stem) increase faster than those farther away (Fig. 8). Moreover, the first three shells contribute more to the whole volume and contain more vessels than the last three shells. The fast pressurization in the shells nearer to surface explains the fast pressurization from 30 kPa to about 60 kPa in less than 1 h, and the slow pressurization in the following measurements can be attributed to the vessels farther from the surface of the stem. This also explains why the initial bubble pressures after 0.6 h were higher in Figure 3 than expected by figure 1 in Wang et al., 2015.

The slow average equilibration rate of bubble pressure in Figure 8 (line) had a time constant of about 18.2 h for diffusional times from 1 to 10 h and was very close to the experimentally determined time constant (17.1 ± 3.3 h) shown in Figure 5 for *Populus* 84K. Hence, experimental results in Figure 5 were confirmed by theoretical expectations.

Another way of looking at the rapid equilibration near the surface is to look at a catena model. In the catena model, we talk about diffusion of gases between embolized vessels, where the rate limitation is diffusion through adjacent cell wall (especially pit membranes). These ideas are developed in Supplemental Appendix S2 but are rather fanciful, because it combines many

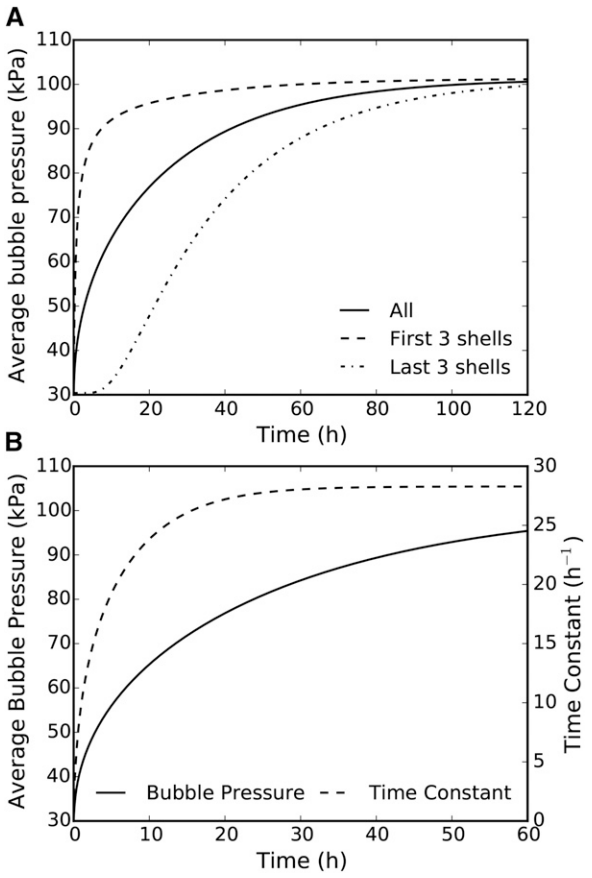

Figure 8. This figure shows the theoretical average bubble pressure in a cylindrical woody stem. The stem was divided into 20 cylindrical shells. The lines, dashed lines, and dash-dot lines represent the volume-based average bubble pressure in all of the 20 shells, the first 3 shells nearest to the stem surface, and the last 3 shells in the center of the stem. A shows results for 120 h. B shows results for the first 60 h and the time constants versus time (dashed line).

serial embolized vessels in a chain; as a model, it is less defined, because many of the parameters used and the structure of the wood (locations and connectivity of embolized vessels) are unknown (Zimmermann and Tomlinson, 1965; Larson, 1975; Tyree and Zimmermann, 2002). This model is presented in Supplemental Appendix S2, but we feel that the processes involved in a catena model are included when the average D_w is measured in wood samples (Sorz and Hietz, 2006); hence, a separate account is not required in our models.

The Impact of a Variable Diffusion Coefficient on Pressurization Rate

The pressurization rate of bubbles in cavitated vessels can be greatly influenced by the diffusion coefficient of the gases in wood (D_w), which defines the penetration rate of air through the wood. Sorz and Hietz, (2006) investigated the relationship between D_w and the air content in xylem; figure 3 in Sorz and Hietz, 2006 showed that D_w is positively correlated to the air content in xylem and that D_w for radial diffusion increased by about a factor of 10 as xylem-air content changed from 0% to 20%. The D_w used in our model is 1E-6 $cm^2\ s^{-1}$, which is the empirical value when gas content is near 10%. The D_w ought to be lower than 1E-6 $cm^2\ s^{-1}$ if PLC = 50% in *A. mono* and *Populus* 84K, where the air contents are around 4.3% and 7.6%, respectively. As PLC increases, the D_w in xylem ought to increase. The increase in D_w makes the gas diffusion faster, and hence, the bubble pressurization is accelerated. This acceleration is illustrated by the double-headed arrows in Figure 3. The increase in D_w in higher PLC stems would cause the higher bubble pressure measured after 1 h and at later times. The reason that D_w in water-saturated wood is lower than in pure water is because suberized regions of cell walls have quite low D_w values. The reason for the increase of D_w as air fraction in wood increases is slightly more complex. The D_w is an average value of all phases (gas, liquid, and solid). The gas diffusion in solids is very near zero, but the gas diffusion coefficient in gas is 10^5 times more than gas diffusion in water. Hence, the average value for radial D_w in wood is quite sensitive to the gas fraction, which is randomly distributed through the volume. The increase in D_w as PLC increases can explain the higher than expected values on the right sides of the plots in Figure 3.

The dependence of D_w on gas fraction is most clearly confirmed by Figure 3 but is not obvious from Figure 5, which applies to times from 1 to 10 h. The reason for this deserves more study, but for now, a probable explanation is that repeated measurements of k_h to bubble pressure accelerate the pressurization of bubbles, because injection of water to measure k_h also injects air; when the volume fraction of air is low, the acceleration to equilibrium is faster than when the volume fraction of air is high. Therefore, this tends to flatten out the trend line in Figure 5. If air injections did not add air to bubbles, the slope in Figure 5 should be negative. However, it takes fewer injections to fully pressurize bubbles on the left side in Figure 5 than on the right side. It was also necessary to inject water periodically to compensate for evaporation, and all of these injections will distort the kinetics.

Theoretical Impact of Bubble Pressure on VCs and the Estimation of P_{50}

The measurement of k_h in cavitated stems will always increase with increasing fluid pressure; in theory, this happens even if the P_b* is at atmospheric pressure, because increasing fluid pressure and surface tension will compress the bubbles and slowly dissolve the bubbles. Therefore, flushing stems under high pressure is a standard method of removing air bubbles. Therefore, in theory, measuring k_h with water under tension will always measure a more realistic value of k_h (i.e. a value closer to daytime values in planta when xylem pressure is well below atmospheric pressure). It also follows that

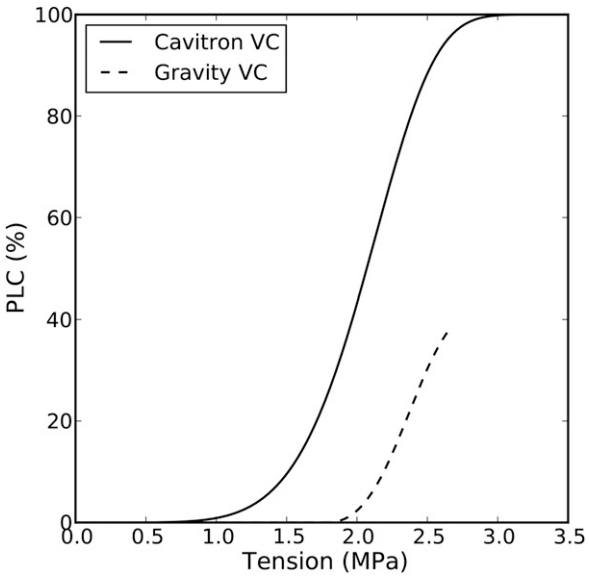

Figure 9. Theoretical comparison between two methods of measuring VCs: gravity VC and cavitron VC. Gravity VC is constructed by plotting PLC measured near atmospheric pressure estimated by using average bubble pressure derived from two point fitting in *Populus* 84K from Figure 2. The cavitron VC was constructed by using a single Weibull curve, of which *b* and *c* are 2.2 and 6, respectively. For details, see "Discussion."

native PLC values will be slightly underestimated when measured in a conductivity apparatus versus when measured in a relative negative pressure. Centrifuges have been commonly used to induce embolism since 1997 (Alder et al., 1997; Li et al., 2008; Hacke et al., 2015). The Sperry technique uses a rotor to induce embolisms, but the k_h and PLC are measured at fluid pressures 1 or 2 kPa above atmospheric pressure. In contrast, when the Cochard rotor is used, the rotor is used for both inducing embolism and measuring k_h and PLC under negative pressure (Cochard, 2002; Cochard et al., 2005).

How much might these factors influence VCs of *Populus* 84K? Results of *Populus* 84K, shown as the regression line in Figure 3B, were used to compute the gravity PLC curves theoretically as shown in Figure 9, which is the worst case. The cavitron VC is built by using average Weibull fitting constants, *b* and *c*, of more than six stems to construct the line in Figure 9. To construct the dashed line in Figure 9, we (1) took PLC values at each cavitron tension value (line), (2) computed the bubble pressure from the best fit line in Figure 3B, and (3) computed the bubble compression and k_h that would result from gravity k_h measurements using equation 6 in Wang et al., 2015. The P_{50} can be shifted by 0.6 MPa in the above calculation, but we are guessing that the real error might be as little as 0.2 MPa. More research is needed to determine the actual error in P_{50} obtained by the Sperry versus Cochard methods. The traditional bench-top dehydration method is likely to produce a P_{50} that is more realistic, because during the time of bench-top dehydration, more time is allowed for exogenous equilibration and more open vessels accelerate the gas transfer deep into the xylem.

Li et al. (2008) compared mean values of P_{50}, P_{63}, and specific conductivity of 10 different species by the spin and gravity methods, which are similar to comparing the *x* axis shifts in the two curves in Figure 9. We have eliminated from this list the conifer species that are not addressed in this study and may or may not be as sensitive as vessel to the impact of the pressure on k_h values. We also eliminated from consideration species with long vessels, which are thought to bias P_{50} and P_{63} values (Cochard et al., 2013; Wang et al., 2014a). The means of P_{50} and P_{63} values were generally based on n = 6 measurements. Owing to the high level of SE of these measurements, there was no significant difference in three of five short-vessel species. However, two of five diffuse porous species had significantly different P_{50} or P_{63} values differing by about 0.3 to 0.6 MPa in a direction that is consistent with the estimates in Figure 9. Therefore, there is ample justification for more research.

The results of this study and the study by Wang et al. (2015) prove that the two methods ought to produce different results, but more work really needs to be done to determine the magnitude of the differences. The answer is still indeterminate, although data in this article provided evidence that the tempo of P_b* change from exogenous sources has an equilibrium time >24 h in most cases. The reason why the answer is quantitatively indeterminate is because it is hard to predict how much air is transported into the stem during measurement in the conductivity apparatus. If the water injected is degassed, then the measurement process will remove gas from bubbles and increase k_h. However, if the water used in the conductivity apparatus is saturated with air at standard barometric pressure, but the bubbles are at, say, 60 kPa, then the process of making measurements will decrease k_h each time that the sample is removed from the Sperry rotor to measure k_h; this is because exogenous air is added to the stem each time that air-saturated water is used to determine k_h.

Future work to resolve this question would require measuring the concentration of air in the solution used in the conductivity apparatus and cavitron, measuring the total volume of water perfused through the stem to measure k_h, and comparing these volumes and concentrations with the volume of air bubbles in the stem and the volume of water in the stem. During measurements, the endogenous equilibrium would be quite fast (1 min; Supplemental Fig. S1), but the speed of exogenous equilibrium could be increased depending on the exact protocol of k_h measurements.

CONCLUSION

In conclusion, the results were consistent with the notion that about 1 d is needed for bubble pressure equilibrium to reach atmospheric values; hence, further study should take the bubble pressure into account

when interpreting VCs and k_h values measured in the first 1 h after cavitation. Errors are likely to be larger when VCs and k_h are measured with a conductivity apparatus than when they are measured in a Cochard rotor. Therefore, we recommend that people measure the VC in cavitron to avoid bubble collapse and make proper correction for background flow when measuring k_h values in a conductivity apparatus (gravity method). More research directed toward quantifying the errors in the conductivity apparatus seems justified to better quantify the impact on P_{50} measured by the two methods, because values do differ for some species (Li et al., 2008), and our analysis provides a basis to understand the physical reasons for these differences.

MATERIALS AND METHODS

Plant Materials

Acer mono 'Maxim' and a hybrid *Populus* 84K (*Populus alba* × *Populus glandulosa* 'Uyeki') were used to study the tempo of bubble formation. The experiments were conducted in the fall of 2013 and summer of 2014. Branches >1-m long were collected in or near the campus of Northwest A & F University (34° 15′ N, 108° 4′ E; altitude of 457 m). Stems with high hydraulic conductivity were preferred in this study, because most of the experimental measurements were done under low tension with low flow rate. Therefore, big diameter stems (8–10 mm) were preferred because of their higher conductance, and then bark was removed from the basal 15 to 20 mm to obtain a basal diameter of 6 to 8 mm to fit into the cavitron reservoir (10 × 10 mm^2). Stems were cut into 27.4-cm segment lengths under water. The water used for flushing and measuring k_h was degassed with 10 mM KCl, which was filtered with a 0.02-μm filter. The stems were flushed under 200 kPa (300 kPa absolute pressure) for 30 min to remove embolism and air bubbles before conducting any experiment. The average vessel lengths and vessel diameters of *A. mono* and *Populus* 84K are 1.95 and 6.42 cm and 20.1 and 28.7 μm, respectively.

Hydraulic Conductance Measurements in the Cavitron

A modified Cochard rotor (Xiangyi; model H2100R) was used to induce embolism and measure hydraulic conductivity of stems. A more precise regression method together with better temperature controlling was essential to measure small changes in hydraulic conductance precisely (Wang et al., 2014b). Briefly, the temperature of the cavitron was set to 25°C, and it was spun for 20 min to obtain a stable temperature in the centrifuge before experiments began. Flushed stem was put into the cavitron and spun at 1,000 rpm (T_c = 0.088 MPa) for 15 min to stabilize before measuring its maximum hydraulic conductance, k_{max}. After measuring k_{max}, a high revolutions per minute was applied to increase the tension in one step. Stems were spun under high tension to induce embolism, and then a series of k_h values was measured to estimate the bubble pressure in the stem (Wang et al., 2015). For each k_h measurement, a series of points after injecting 10 mM KCl was collected and then used to compute k_h with the regression method (Wang et al., 2014b).

Bubble Pressure Estimations by Multipoint and Two-Point Methods and Stems PLC

The k_{max} values of stems were measured at 1,000 rpm after 15 min of temperature stabilization, and then the tension was increased to a high central tension immediately to induce embolism. The high central tension values ranged from 4.0 to 4.5 MPa and 2.0 to 2.5 MPa for *A. mono* and *Populus* 84K respectively, to induce PLC ranges from 20% to 90%. Stems were spun under high tension, and embolism was induced for 20 min; then the hydraulic conductivity at high tension, k_{hh}, was measured. Tension was reduced to 0.0565 MPa (800 rpm); k_h was measured repeatedly to document the approach to equilibrium ("Results"), and the tension was held constant for 40 min to allow pressure equilibrium in vessels. During the 40-min interval, 10 mM KCl liquid was injected into the two reservoirs every 5 min to replenish the water absorbed by the stem. Hydraulic conductivity at low tension, k_{hl}, was measured at 800 rpm, and then the revolutions per minute were increased stepwise to 900, 1,000, 1,200, 1,400, 1,600, 1,800, 2,000, 2,500, and 3,000, etc. After a 5-min wait period at each higher tension, the k_h was measured. A series of hydraulic conductivity measurements was collected to construct a hydraulic recovery curve and hence, estimate the average bubble pressure in the stem with the hydraulic recovery model described in Wang et al., 2015.

The values measured at the highest and lowest tensions were chosen to compute average bubble pressure with two-point fitting. The two points were k_{hh} measured under high tension and k_{hl} measured under 0.0565 MPa. Average bubble pressures estimated from two-point fitting and curve fitting were compared with values obtain by fitting the entire curve.

Kinetics of Bubble Collapse after Tension Reduction and the Measurement of the Long-Term Pressurization

Hydraulic conductivity kinetics experiments were done on *Populus* 84K. After k_{max} was measured, the stem was spun under high tension, $T_{c,h}$, for 20 min to induce embolism. After the 20-min spin under high tension, k_{hh} was measured, and the tension was decreased to 0.0565 MPa in one step. The stem ought to absorb water because of bubble collapse, and the water absorption would cause changes in the estimation of conductivity. Therefore, hydraulic conductivity was measured under low tension every 2 to 3 min until stable, and the stable value was saved as k_{hl} to estimate the bubble pressure in the stem. After k_{hl} was measured, tension was increased to $T_{c,h}$ in one step, and then the stem was spun for 1 h. It is necessary to add 10 mM KCl liquid periodically to the reservoirs to replenish the water evaporated; otherwise, the cuvette will become empty. Hydraulic conductivity was measured, and then the tension was reduced to 0.0565 MPa to measure k_h continuously to obtain k_{hl}. The high tension to low tension process was repeated every 2 h to obtain four to five k_{hl} measurements to study bubble pressurization in stems. The entire progress takes 8 to 10 h.

Program and Statistics

The model to estimate bubble pressure was programed by Python(x,y) 2.7.9, and the fittings were done by the least-square package in Python. The statistics were done by the scipy packages in Python.

Supplemental Data

The following supplemental materials are available.

Supplemental Figure S1. Equilibrium time of endogenous diffusion.

Supplemental Theory S1. Correction of diffusion coefficient.

Supplemental Appendix S1. Radial diffusion model.

Supplemental Appendix S2. Catena model.

ACKNOWLEDGMENTS

We thank Feng Feng for valuable help in collecting samples and maintaining the flushing apparatus.

Received June 10, 2015; accepted October 14, 2015; published October 14, 2015.

LITERATURE CITED

Alder NN, Pockman WT, Sperry JS, Nuismer S (1997) Use of centrifugal force in the study of xylem cavitation. J Exp Bot **48:** 665–674

Cai J, Hacke U, Zhang S, Tyree MT (2010) What happens when stems are embolized in a centrifuge? Testing the cavitron theory. Physiol Plant **140:** 311–320

Cochard H (2002) A technique for measuring xylem hydraulic conductance under high negative pressures. Plant Cell Environ **25:** 815–819

Cochard H, Badel E, Herbette S, Delzon S, Choat B, Jansen S (2013) Methods for measuring plant vulnerability to cavitation: a critical review. J Exp Bot **64:** 4779–4791

Cochard H, Damour G, Bodet C, Tharwat I, Poirier M, Améglio T (2005) Evaluation of a new centrifuge technique for rapid generation of xylem vulnerability curves. Physiol Plant **124:** 410–418

Crank J (1979) The Mathematics of Diffusion, Ed 2. Oxford University Press, Oxford

Hacke U, Sperry J, Pittermann J (2000) Drought experience and cavitation resistance in six shrubs from the Great Basin, Utah. Basic Appl Ecol **1:** 31–41

Hacke UG, Venturas MD, MacKinnon ED, Jacobsen AL, Sperry JS, Pratt RB (2015) The standard centrifuge method accurately measures vulnerability curves of long-vesselled olive stems. New Phytol **205:** 116–127

Irvine J, Grace J (1997) Continuous measurements of water tensions in the xylem of trees based on the elastic properties of wood. Planta **202:** 455–461

Larson PR (1975) Development and organization of the primary vascular system in Populus deltoides according to phyllotaxy. Am J Bot **62:** 1084–1099

Li Y, Sperry JS, Taneda H, Bush SE, Hacke UG (2008) Evaluation of centrifugal methods for measuring xylem cavitation in conifers, diffuse- and ring-porous angiosperms. New Phytol **177:** 558–568

Sorz J, Hietz P (2006) Gas diffusion through wood: implications for oxygen supply. Trees **20:** 34–41

Sperry JS, Tyree MT (1988) Mechanism of water stress-induced xylem embolism. Plant Physiol **88:** 581–587

Torres-Ruiz JM, Sperry JS, Fernández JE (2012) Improving xylem hydraulic conductivity measurements by correcting the error caused by passive water uptake. Physiol Plant **146:** 129–135

Tyree MT, Yang S (1992) Hydraulic conductivity recovery versus water pressure in xylem of *Acer saccharum*. Plant Physiol **100:** 669–676

Tyree MT, Zimmermann MR (2002) Xylem Structure and the Ascent of Sap. Springer, Berlin

Wang R, Zhang L, Zhang S, Cai J, Tyree MT (2014a) Water relations of Robinia pseudoacacia L.: do vessels cavitate and refill diurnally or are R-shaped curves invalid in Robinia? Plant Cell Environ **37:** 2667–2678

Wang Y, Burlett R, Feng F, Tyree MT (2014b) Improved precision of hydraulic conductance measurements using a Cochard rotor in two different centrifuges. J Plant Hydraul **1:** e0007

Wang Y, Pan R, Tyree MT (2015) Studies on the tempo of bubble formation in recently cavitated vessels: a model to predict the pressure of air bubbles. Plant Physiol **168:** 521–531

Yang S, Tyree MT (1992) A theoretical model of hydraulic conductivity recovery from embolism with comparison to experimental data on Acer saccharum. Plant Cell Environ **15:** 633–643

Zhou H, Sun Y, Tyree MT, Sheng W, Cheng Q, Xue X, Schumann H, Schulze Lammers P (2015) An improved sensor for precision detection of in situ stem water content using a frequency domain fringing capacitor. New Phytol **206:** 471–481

Zimmermann MH, Tomlinson PB (1965) Anatomy of the palm Rhapis excelsa, sc. I. Mature vegetative axis. J Arnold Arbor **46:** 160–178